Mobility of symmetric block-and-hole polyhedra☆

Simon D. Guest[a], Patrick W. Fowler[b], Bernd Schulze[c],*

[a] *Department of Engineering, University of Cambridge, Trumpington Street, Cambridge CB2 1PZ, UK*
[b] *Department of Chemistry, University of Sheffield, Sheffield S3 7HF, UK*
[c] *Department of Mathematics and Statistics, Lancaster University, Lancaster LA1 4YF, UK*

ABSTRACT

Block-and-hole polyhedra can be derived from a bar-joint triangulation of a polyhedron by a stepwise construction: select a set of non-overlapping disks defined by edge-cycles of the triangulation of length at least 4; then modify the interior of each disk by an addition or deletion operation on vertices and edges so that it becomes either a rigid block or a hole. The construction has a body-hinge analogue. Models of many classical objects such as the Sarrus linkage can be modelled by block-and-hole polyhedra. Symmetry extensions of counting rules for *mobility* (the balance of mechanisms and states of self-stress) are obtained for the bar-joint and body-hinge models. The extended rules detect mechanisms in many cases where pure counting would predict an isostatic framework. Relations between structures where blocks and holes are swapped have a simple form. Examples illustrate the finer classification of isostatic and near-isostatic block-and-hole polyhedra achievable by using symmetry.

The present approach also explains a puzzle in standard models of mobility. In the bar-joint model, a fully triangulated polyhedron is isostatic, but in a body-hinge version it is heavily overconstrained. When the bodies are panels with hinge lines intersecting at vertices, the overconstraints can be explained in local mechanical terms, with a direct symmetry description. A generalisation of the symmetry formula explains the extra states of self-stress in panel-hinge models of block-and-hole polyhedra.

1. Introduction

As structures poised between mobility and over-bracing, just-rigid isostatic frameworks are of perennial interest in engineering applications (Maxwell, 1876; Bujakas and Rybakova, 1998; Stewart, 1965; Miura et al., 1985; Baker and Friswell, 2009). Fully triangulated (strictly convex) polyhedra are guaranteed by the Cauchy–Dehn Theorem to be isostatic (Cauchy, 1813; Dehn, 1916). Furthermore, Gluck showed in 1975 that the graph of any triangulated sphere is generically isostatic in 3-space (Gluck, 1975). Bar-joint frameworks based on triangulated spheres therefore provide good starting points for exploration of isostatic and related structures. Indeed, removal of just one edge of such a framework is sufficient to give a finite mechanism (Maxwell, 1890).

One class of structures currently attracting attention in the literature of rigidity is that of block-and-hole frameworks (Finbow-Singh et al., 2012; Finbow-Singh and Whiteley, 2013; Cruickshank et al., 2017), which can model situations such as geodesic domes pierced by windows, or open-ended tubular tower-like structures. Mathematical work has concentrated on general combinatorial characterisations of rigidity (Whiteley, 1988; Finbow-Singh and Whiteley, 2013; Cruickshank et al., 2017). Work on applications needs to reach an understanding of particular geometric realisations of such structures, especially those with non-trivial symmetries. In these cases, pure counting does not always reveal mechanisms, and indeed other types of 'perforated polyhedra' (Fowler et al., 2016) may possess unexpected mechanisms that are only understood by use of symmetry-extended counting rules.

Here we extend 'counting with symmetry' (Fowler and Guest, 2000; Guest and Fowler, 2005; Connelly et al., 2009) to the mobility of block-and-hole frameworks, and show that this approach can give useful information on candidates for isostatic frameworks, and on properties of structures related by swapping blocks and holes (Finbow-Singh et al., 2012).

We work with *block-and-hole polyhedra*, which we take here to be structures derived from a bar-joint triangulation of the sphere by selecting a set of non-overlapping disks defined by cycles of length at least four composed of edges of the triangulation, followed by modification of each disk so that it becomes either a
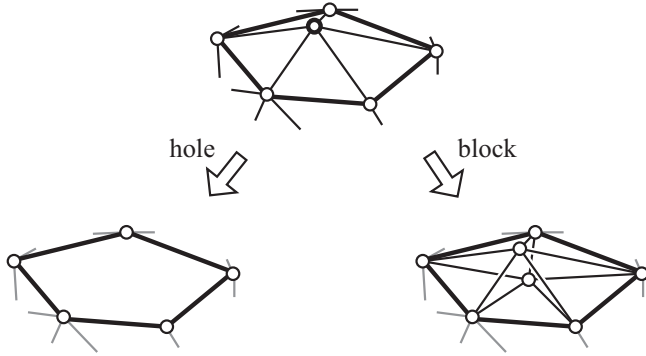
Fig. 1. Construction of a hole and a rigid block (a panel) from a bar-joint triangulation of the sphere.

rigid block or a hole. Edges making up a chosen cycle are not necessarily coplanar. With our definition, we are choosing to consider the structures that can be formed by a series of independent hole-punching and block-rigidifying operations. This simplifies the symmetry arguments and allows us to reach a general equation for mobility of block-and-hole polyhedra (because vertices and edges at hole boundaries are restricted to trivial rotational symmetries). We focus on 'counting-isostatic' block-and-hole polyhedra, where the standard mobility count $m - s$ is equal to zero. However, the approach is equally able to describe over-braced or under-braced block-and-hole systems, where a swap of blocks and holes simply changes the sign of the mobility count. In the symmetry-extended formulation, this swap may have consequences for the finite or infinitesimal nature of predicted mechanisms.

Block-and-hole polyhedra may take various forms, as, for example, panel-hinge frameworks (Katoh and Tanigawa, 2011) in the case where the vertices of each block are coplanar and holes do not share any vertex. In such a structure, blocks are flat panels that are connected in pairs along edges which function as hinges that allow a rotational motion of one panel around the other. Useful panel-hinge physical models of block-and-hole polyhedra can be created with commercial kits (Polydron, 2016), as shown in figures in the present paper. Switching between bar-joint and panel-hinge models brings to light an interesting "puzzle": the apparently equivalent panel-hinge model has more states of self-stress. We explore the origin of these states, and show that they can be counted, assigned symmetries and explained with a simple localised mechanical model.

The structure of the paper is as follows. In Section 2 a bar-joint model of block-and-hole polyhedra is described in terms of operations performed on an initially fully triangulated framework. A symmetry-extended counting rule is given for the mobility of the bar-joint model. In Section 3 the corresponding panel-hinge model is presented and the symmetry-extended counting rule is derived and the puzzling 'extra' states of self-stress are explained. In Section 4, examples bring out the rich behaviour of different kinds of block-and-hole polyhedra, all undetected by scalar counting. Finally, in Section 5 we discuss briefly how the methods of this paper may be applied to other types of block-and-hole structures.

2. A bar-joint model for block-and-hole polyhedra

In our approach, we model any given block-and-hole polyhedron by a series of successive applications of operations of two types to a bar-joint triangulation of a topological sphere (which is not necessarily convex) (Fig. 1).

One operation generates a *hole* by removal of a vertex v_h along with its incident edges from the original triangulation. The other operation generates a *block* by identifying a vertex v_b of degree

$d(v_b) \geq 4$ in the original triangulation and duplicating it (coning over the neighbours of v_b); this forms a $[d(v_b)]$-bipyramid, which is guaranteed to be isostatic in generic geometry by Gluck's theorem (Gluck, 1975). We choose a position for the duplicate vertex (and slightly perturb the position of v_b if necessary) in such a way that the coned system is in fact isostatic in 3-space.

2.1. Scalar and symmetry-extended counting rules

A 3D bar-joint framework with b bars and j joints has m mechanisms and s states of self-stress and obeys the Maxwell Rule (Maxwell, 1864; Calladine, 1978).

$$m - s = 3j - b - 6. \tag{1}$$

In the symmetry extension (Fowler and Guest, 2000) for a bar-joint framework with point group $\mathcal{G}$, the counting equation becomes

$$\Gamma(m) - \Gamma(s) = \Gamma(j) \times \Gamma_T - \Gamma(b) - (\Gamma_T + \Gamma_R), \tag{2}$$

or, in terms of the underlying graph with v vertices and e edges:

$$\Gamma(m) - \Gamma(s) = \Gamma(v) \times \Gamma_T - \Gamma(e) - (\Gamma_T + \Gamma_R). \tag{3}$$

In the terminology of mathematical group theory, each Γ in these equations is the character of a group representation of $\mathcal{G}$. A group representation of $\mathcal{G}$ is a homomorphism from $\mathcal{G}$ to the general linear group of some vector space, and the character of the representation associates to each group element the trace of the corresponding matrix. In applied group theory, what is called a character in the mathematical formulation is usually called a representation, and the trace under an operation is called the character, and this is the terminology we will use below. In this applied context, the Maxwell Rule (1) is simply the *character* of the symmetry equation (2) under the identity operation. For point groups in 3-space and their irreducible representations, we will use the standard Schoenflies and Mulliken notations, respectively (Altmann and Herzig, 1994; Atkins et al., 1970).

In our equations, $\Gamma(m)$ and $\Gamma(s)$ are the *representations* of the mechanisms and states of self-stress of the framework. For any set of objects q, $\Gamma(q)$ is the permutation representation of q; that is, the entry of the representation $\Gamma(q)$ corresponding to a group element $x \in \mathcal{G}$ is equal to the number of objects in the set that remain unshifted by the symmetry operation x. In addition, Γ_T and Γ_R are three-dimensional translational and rotational representations, respectively. Two representations that will be useful later are Γ_0 and Γ_ϵ, respectively the totally symmetric and determinantal representations: Γ_0 is the symmetry of an object that is preserved under all symmetry operations; Γ_ϵ is the symmetry of an object that is preserved under all proper, and reversed under all improper symmetry operations. Useful relations are $\Gamma_\epsilon \times \Gamma_\epsilon = \Gamma_0$ and $\Gamma_R = \Gamma_T \times \Gamma_\epsilon$.

All the representations in (2) and (3) can be computed by standard manipulations of the character table of the group $\mathcal{G}$ (Altmann and Herzig, 1994; Atkins et al., 1970). Note that $\Gamma(m) - \Gamma(s)$ is typically a reducible representation, i.e., a linear combination in which those irreducible representations that occur with positive coefficients describe symmetries of mechanisms, and those with negative coefficients describe symmetries of states of self-stress.

The equation $m - s = 0$ is a necessary but not sufficient condition for a structure to be isostatic. (A structure can have mechanisms and states of self-stress that cancel in the count.) The symmetry extension can be seen as a set of additional necessary conditions, one for each class of operations in the point group. This is typically more informative than the scalar rule, which is just the character of (2) under one operation. We refer to those mechanisms and states of self-stress that cannot be detected using the

scalar rule (1) but are revealed by the symmetry-extended counting rule (2) as *symmetry-detectable*.

2.2. Symmetry aspects of the construction

The construction described above yields a bar-joint framework that differs from the original triangulation in two obvious respects: the presence of blocks and of holes. In symmetry terms, the effect in (3) of deleting a set of vertices $\{v_h\}$ and their incident edges $\{e_h\}$ at the hole sites is to subtract a term $\Gamma(v_h) \times \Gamma_T - \Gamma(e_h)$ from $\Gamma(m) - \Gamma(s)$. Likewise, the addition of vertices $\{v_b\}$ and their edges $\{e_b\}$ at the block sites adds a term $\Gamma(v_b) \times \Gamma_T - \Gamma(e_b)$ to $\Gamma(m) - \Gamma(s)$. Typically the process of creation of blocks and holes will reduce the overall symmetry; calculations of the various representations are understood to take place in the smaller point group appropriate to the block-and-hole system.

Given that by construction we start from an isostatic structure, the *total* mobility of the bar-joint block-and-hole structure is given by the difference term:

$$[\Gamma(m) - \Gamma(s)]_{BH} = [\Gamma(v_b) - \Gamma(v_h)] \times \Gamma_T + [\Gamma(e_h) - \Gamma(e_b)]. \quad (4)$$

This is our main working equation. It will be used to deduce the mobility properties of all the various block-and-hole structures to be described in the examples below.

Some remarks follow straightforwardly.

(i) The trace of symmetry equation (4) under the identity operation is simply the scalar count, and hence

$$(m - s)_{BH} = 3(|v_b| - |v_h|) + (|e_h| - |e_b|),$$

or in terms of vertices $v_{h_1}, \ldots, v_{b_1}, \ldots$ with degrees $d_{h_1}, \ldots, d_{b_1}, \ldots$,

$$(m - s)_{BH} = \sum_{i=1}^{|v_h|}(d_{h_i} - 3) - \sum_{i=1}^{|v_b|}(d_{b_i} - 3),$$

consistent with the fact that the structure would retain its isostatic count $m - s = 0$ if all blocks and holes were based on triangles: the isostatic count persists for all symmetry operations, since $\Gamma(v_X) \times \Gamma_T = \Gamma(e_X)$ for each set of trivalent vertices with their associated edges (X = b or h), and hence $(\Gamma(m) - \Gamma(s))_{BH}$ vanishes in this case.

(ii) As much of the interest in block-and-hole frameworks lies in their potential as isostatic structures, it seems useful to define a notion of *balance* for bar-joint block-and-hole frameworks.

At the level of scalar counting, a bar-joint block-and-hole framework with a zero count $(m - s)_{BH}$ will be called *counting-isostatic*. The count of zero can be achieved in various ways. A case in which $|v_h| = |v_b|$ and $|e_h| = |e_b|$ will be called *counting-balanced*. The special case in which every hole vertex has a corresponding block vertex of the same degree will be called *strongly counting-balanced*.

At the level of counting with symmetry, more situations are possible. Not all structures with $m - s = 0$ have $\Gamma(m) - \Gamma(s) = 0$. A zero representation $(\Gamma(m) - \Gamma(s))_{BH}$ implies that neither mechanisms nor states of self-stress are detectable by symmetry. We will call this case *symmetry-counting-isostatic*, or *symmetry-isostatic* for short. A way to achieve vanishing of $(\Gamma(m) - \Gamma(s))_{BH}$ is to have $\Gamma(v_b) = \Gamma(v_h)$ and $\Gamma(e_b) = \Gamma(e_h)$. This case is *symmetry-counting-balanced*, or *symmetry-balanced*. A specific way to ensure this symmetry balance is to *start* with a counting-balanced structure and to choose $\{v_h\}$ and $\{v_b\}$ such that the two sets of vertices and the two sets of edges $\{e_h\}$ and $\{e_b\}$ span the same combinations of orbits of the point group

of the derived structure (Fowler and Quinn, 1986). By analogy with the symmetry-free terminology, we will call this case *strongly symmetry-counting-balanced*, or simply *strongly symmetry-balanced*.

The point of this hierarchy of definitions is that counting with symmetry is intrinsically more discriminating than scalar counting. In particular:

(a) Symmetry-isostatic implies counting-isostatic;
(b) Symmetry-balanced implies counting-balanced;
(c) Strongly symmetry-balanced implies strongly counting-balanced.

Within each stack of scalar or symmetry counting, strongly balanced implies balanced implies isostatic. The gap between symmetry and simple counting at each level can lead to cases where a bar-joint framework is isostatic according to counting but has symmetry-detectable mechanisms and states of self-stress (see examples below).

(iii) Both symmetry-extended and scalar mobility equations are evidently *anti-symmetric* with respect to exchange of blocks and holes. With the scalar equation, the prediction is simply that the excess of mechanisms over states of self-stress will be reversed. With the symmetry-extended equation, the prediction is more subtle: symmetries of excess mechanisms and states of self-stress will be swapped and this may lead to physically distinguishable consequences. Given the symmetry rules governing finiteness of mechanisms (Guest and Fowler, 2007), the change in symmetry may lead to blocking of mechanisms in one case but not the other. Examples given later illustrate these possibilities.

3. A panel-hinge model for block-and-hole polyhedra

Consider a 3D structure consisting of rigid bodies connected in pairs by joints that allow various degrees of freedom. Such a structure with m mechanisms and s states of self-stress obeys the well-known Kutzbach–Grübler mobility criterion (Grübler, 1917; Kutzbach, 1929). This scalar counting equation can be extended to a symmetry relation by using the concept of a contact polyhedron C, in which bodies are associated with vertices and joints with edges. The general approach is described elsewhere (Guest and Fowler, 2005).

For the particular case of a body-hinge structure consisting of p bodies and h hinges, where each hinge allows only one relative degree of freedom between the two bodies it connects, the standard Kutzbach–Grübler counting relation is

$$m - s = 6p - 5h - 6 \quad (5)$$

and the symmetry-extended form of this relation is

$$\Gamma(m) - \Gamma(s) = (\Gamma_T + \Gamma_R) \times [\Gamma(v, C) - \Gamma_\parallel(e, C)] - (\Gamma_T + \Gamma_R) + \Gamma_h. \quad (6)$$

The representation $\Gamma_\parallel(e, C)$ refers to vectors along edges of C, and Γ_h refers to the freedoms associated with the hinges. Further details are available elsewhere (Guest and Fowler, 2005; Fowler et al., 2016).

Up to this point, we have been using a bar-joint framework model for block-and-hole structures which can be analysed using the Maxwell Rule. There is a corresponding *body-hinge* framework, which can be formed from the bar-joint framework as follows: replace each [d]-bipyramid by a d-sided 'panel' and each remaining triangular face by a triangular panel; connect the panels together by hinges that allow rotational motion about the line of the edge of the underlying triangulation of the sphere.

'Panel' here has the intuitive definition used in the engineering context: a rigid body with boundary defined by a cycle of
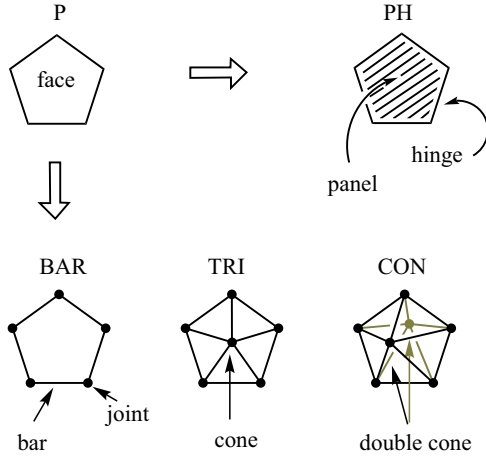
Fig. 2. A set of objects related to the polyhedron $\mathcal{P}$: a panel-hinge model of $\mathcal{P}$ (PH); a bar-joint model of the polyhedron (BAR); a fully triangulated bar-joint polyhedron (TRI); a double-cone construction of a bar-joint model with blocks for all faces (CON).

hinges and/or hole edges. In the mathematical literature it is usually considered that panels are planar, with coplanar hinge lines, but coplanarity is not assumed in the construction used in the present work. Instead, a panel in this paper only has the special property that successive hinge edges on its boundary always lie on intersecting lines. The key non-generic feature implied by the use of a spherical triangulation in our underlying construction is that the hinge lines between panels around a vertex all pass through that vertex. A surprising consequence of this is discussed below.

3.1. The puzzle of additional states of self-stress in panel-hinge structures

As we are switching between different representations of frameworks based on triangulations, it is useful to note a potentially confusing distinction between a polyhedron constructed from panels and hinges and the same polyhedron rendered as a bar-joint framework. This distinction extends to the corresponding physical models of the derived block-and-hole polyhedra. In short, the panel-hinge models have more states of self-stress. We show here that these can be characterised by number and symmetry, and we provide a mechanical explanation of their localised nature.

3.1.1. Scalar counting

To discuss the differences between the panel-hinge and constructed bar-joint models of a block-and-hole framework, it is useful to define a set of objects related to a given 'full' polyhedron (one where *all* faces are blocks). Call this polyhedron $\mathcal{P}$. It has f faces, e edges and v vertices.

The first object, PH, is the panel-hinge structure based on $\mathcal{P}$, with rigid panels for faces of $\mathcal{P}$, and hinges along edges of $\mathcal{P}$. The second is BAR, a bar-joint framework with bars along edges of $\mathcal{P}$ and joints at vertices of $\mathcal{P}$. The next two are derived from BAR: they are TRI, a bar-joint framework based on the triangulation derived from $\mathcal{P}$ by coning every face of $\mathcal{P}$ of size greater than three, and CON, the bar-joint framework found by applying our construction to $\mathcal{P}$ to convert all faces of $\mathcal{P}$ to rigid blocks. CON is constructed by adding another cone to every vertex of TRI that corresponds to a face centre of $\mathcal{P}$ (or, equivalently, by double-coning every non-triangular face of $\mathcal{P}$). Schematically, for some face of $\mathcal{P}$, the objects in the sequence have local structure as shown in Fig. 2. We are interested in the difference in mobility count $(m - s)$ between PH and CON. The observation is that PH has extra states of self-stress compared to CON. We can calculate the differences, us-

ing TRI as a convenient intermediate,

$$(m - s)_{\text{PH}} - (m - s)_{\text{CON}} = \Delta, \tag{7}$$

$$(m - s)_{\text{CON}} - (m - s)_{\text{TRI}} = \Delta_1, \tag{8}$$

$$(m - s)_{\text{TRI}} - (m - s)_{\text{BAR}} = \Delta_2, \tag{9}$$

and described in an *ad hoc* notation where $(m - s)_{\text{OBJ}}$ refers to the mobility count of object OBJ. Δ, Δ_1 and Δ_2 are negative integers, because coning introduces more states of self-stress than mechanisms. Noting that Maxwell's rule gives

$$\Delta_1 = \Delta_2 = -\sum_{r>3}(r-3)f_r, \tag{10}$$

where f_r is the number of faces of size r in polyhedron $\mathcal{P}$, and the mobility $(m - s)_{\text{TRI}} = 0$, since the TRI structure is a triangulation of the sphere and hence generically isostatic, we have a relation between the mobilities of CON and BAR

$$(m - s)_{\text{CON}} = -(m - s)_{\text{BAR}} = \Delta_1 = \Delta_2, \tag{11}$$

and hence

$$\Delta = (m - s)_{\text{PH}} - (m - s)_{\text{CON}} = (m - s)_{\text{PH}} + (m - s)_{\text{BAR}}. \tag{12}$$

Combining the counting rules (1) and (5), we find (since here $p = f$, $h = e$)

$$\Delta = (6f - 5e - 6) + (3v - e - 6) = -3v. \tag{13}$$

Hence, the general counting result is that a panel-hinge polyhedron where *all* faces are blocks has $3v$ 'extra' states of self-stress compared to a corresponding bar-joint framework made by double coning all the non-triangular faces of $\mathcal{P}$ to make a block-and-hole polyhedron without holes.

To see how this count of three states of self-stress per vertex is modified in the non-trivial case where the block-and-hole polyhedron has some blocks and some holes, take the simplest case, where holes are based on independent (pairwise non-adjacent) faces of $\mathcal{P}$. Consider the constructions PH and CON as operating locally, face-by-face on some fixed subset of faces of the original polyhedron $\mathcal{P}$: $\mathcal{P}$ will then have *block faces* and *hole faces*. We will use the notation PH′, BAR′ and CON′ to indicate structures where fixed subsets of faces of $\mathcal{P}$ have been modified to give holes and blocks.

The scalar counting argument is clear. Each independent single hole of size r changes the mobility count of the panel-hinge structure by $-6 + 5r$ and the mobility count of the constructed framework by $-6 + 2r$, and hence the introduction of each hole adds $3r$ to the (negative) quantity Δ (now defined as a difference between PH′ and BAR′), equivalent to removal from the vertex count of the number of vertices of $\mathcal{P}$ in the hole boundary. The general result for block-and-hole polyhedra constructed with orbits of isolated holes is that Δ is equal to $-3v_{\text{b}}$, where v_{b} counts the vertices of the panel-hinge structure that are not in any hole boundary:

$$(m - s)_{\text{PH}'} - (m - s)_{\text{CON}'} = -3v_{\text{b}}. \tag{14}$$

3.1.2. Counting with symmetry

The counting result (14) can be given a symmetry-extended form by combining previous expressions. In the case of a panel-hinge framework, the mobility criterion (6) can be modified to take account of the known form of the contact polyhedron, C, and the simple form of the freedoms of the hinges. The vertices of $\mathcal{C}$ are the centres of panels, which are (all, or a subset of) faces of an underlying polyhedron P, and the edges of C run perpendicular to those of the polyhedron, so $\Gamma(v, C) = \Gamma(f, P)$, $\Gamma_{\parallel}(e, C) = \Gamma_{\perp}(e, P)$, and $\Gamma_{\text{h}} = \Gamma(e, C) = \Gamma(e, P)$, where f and e may refer to appropriate subsets of faces and edges. Hence, for the panel-hinge framework

PH modelling the block-and-hole polyhedron, the mobility representation is

$$[\Gamma(m) - \Gamma(s)]_{PH} = (\Gamma_T + \Gamma_R) \times (\Gamma(f) - \Gamma_\perp(e) - \Gamma_0) + \Gamma(e). \tag{15}$$

The symmetry version of the scalar equation for Δ is naturally defined as

$$\Gamma(\Delta) = [\Gamma(m) - \Gamma(s)]_{PH} - [\Gamma(m) - \Gamma(s)]_{CON} \tag{16}$$

For the trivial case of the polyhedron with all faces rigid panels, scalar equation (12) becomes an alternative definition of the representation of the difference Δ, through

$$\Gamma(\Delta) = [\Gamma(m) - \Gamma(s)]_{PH} + [\Gamma(m) - \Gamma(s)]_{BAR} \tag{17}$$

and hence

$$\Gamma(\Delta) = \Gamma_T \times (\Gamma(f) - \Gamma_\perp(e) + \Gamma(v)) \\ - 2(\Gamma_T + \Gamma_R) + \Gamma_R \times (\Gamma(f) - \Gamma_\perp(e)). \tag{18}$$

The proof strategy in this section on counting with symmetry will be to compare mobilities of PH and various bar-joint derivatives, first in the absence of holes, and then with holes, to find the effects on the difference term $\Gamma(\Delta)$ of their introduction. We expect that the complicated expression (18) for $\Gamma(\Delta)$ will collapse to something quite simple, given the scalar result (13).

The symmetry-extended Euler Theorem for polyhedra (Ceulemans and Fowler, 1991) gives an expression for $\Gamma_\perp(e)$

$$\Gamma_\perp(e) = \Gamma(f) + \Gamma(v) \times \Gamma_\epsilon - (\Gamma_0 + \Gamma_\epsilon), \tag{19}$$

and hence all face and edge terms cancel from (18) to give

$$\Gamma(\Delta) = -\Gamma(v) \times \Gamma_R. \tag{20}$$

This matches the counting result that three local states of self-stress are present for each vertex of the 'full' (hole-free) panel-hinge structure, when compared to the mobility count for the constructed bar-joint framework.

To track how $\Gamma(\Delta)$ changes on introduction of some specified set of isolated holes (i.e., holes based on pairwise non-adjacent faces of $\mathcal{P}$), we check how the terms in (16) change when PH becomes PH' and CON becomes CON'. Removal of panels from PH reduces both the set of contributing panel centres and the set of panel perimeter edges. Hence,

$$[\Gamma(m) - \Gamma(s)]_{PH'} - [\Gamma(m) - \Gamma(s)]_{PH} \\ = (\Gamma_T + \Gamma_R)(\Gamma(f)_{PH'} - \Gamma(f)_{PH} - \Gamma_\perp(e)_{PH'} + \Gamma_\perp(e)_{PH}) \\ + (\Gamma(e)_{PH'} - \Gamma(e)_{PH}). \tag{21}$$

Likewise, conversion of blocks within CON to holes reduces the set of contributing cone vertices, and the set of 'spoke' edges in the cones, removing one double cone per hole. Hence,

$$[\Gamma(m) - \Gamma(s)]_{CON'} - [\Gamma(m) - \Gamma(s)]_{CON} \\ = (\Gamma_T + \Gamma_R)\big(\Gamma(f)_{CON'} - \Gamma(f)_{CON} - \Gamma_\perp(e)_{CON'} + \Gamma_\perp(e)_{CON}\big) \\ + (\Gamma(e)_{CON'} - \Gamma(e)_{CON}). \tag{22}$$

Notice that the faces of PH transform as single coning vertices of CON, and that the changes in edges for a given hole involve respectively one copy of the perimeter edges but two copies of the spokes. Note also that since the holes are isolated in our construction, we need not distinguish between $\Gamma(e)$ and $\Gamma_\perp(e)$ for edges on hole perimeters as such edges have at best local C_s symmetry.

Collapsing terms, we obtain the representation $\Gamma(\Delta\Delta)$ which describes the change induced in $\Gamma(\Delta)$ by the holes, as

$$\Gamma(\Delta\Delta) = (\Gamma_R - \Gamma_T) \times \Gamma(f_h) - (\Gamma_T + \Gamma_R - \Gamma_0) \times \Gamma(e_{p,h}) + 2\Gamma(e_{s,h}) \tag{23}$$

where f_h is the set of faces of $\mathcal{P}$ replaced by holes, $e_{p,h}$ is the set of perimeter edges bounding holes, $e_{s,h}$ is the set of spoke edges in a triangulation of the holes, (and v_h will be used for the set of vertices in hole perimeters). Further simplification is not necessary as we can show by evaluating characters that this expression is consistent with the intuition that $\Gamma(\Delta)$ will have the form

$$\Gamma(\Delta) = -\Gamma_R \times \Gamma(v - v_h) \tag{24}$$

where the only vertices to be counted in the permutation representation are those that are *not* on the perimeter of any hole. The 'extra' states of the panel-hinge model of a block-and-hole polyhedron therefore span $\Gamma(\Delta)$.

The proof of (24) is straightforward. The only symmetry elements on which hole centres, edges or vertices can lie are the identity, rotational axes (hole centres only) and mirror planes. Under the identity, the trace of $\Gamma(\Delta\Delta)$ is a contribution of $0 - 5r + 2r = -3r$ per hole of size r. Under a rotation C_n, all perimeter and spoke edges shift, and the trace of $\Gamma_R - \Gamma_T$ vanishes, so the total trace is zero. Under reflections, there are three subcases: a hole that is bisected by a mirror plane may be (i) of odd size, (ii) of even size with 2 perimeter edges cut by the plane, or (iii) of even size with 2 perimeter vertices in the plane. The trace of $\Gamma(\Delta\Delta)$ has a contribution of $+1$ in case (i), 0 in case (ii) and $+2$ in case (iii). Hence, the traces coincide with those of $-\Gamma_R \times \Gamma(v_h)$ for all operations, and (24) is proved.

Fig. 3 illustrates the mechanical argument for the association of the 'extra' states of self stress with local rotations. The key is that all the hinge lines associated with panels around a vertex meet at a common point, the vertex itself.

In principle, the subtractive nature of the mobility criteria, in both scalar and symmetry-extended forms, implies that we could have cancelling mechanisms and extra states of self-stress that do not show up in the count of -3 per vertex. However, the fact that the symmetry result $-\Gamma(v) \times \Gamma_R$ is a combination of irreducible representations with all negative coefficients implies that any such 'hidden' sets of mechanisms and states of self-stress would be equi-symmetric as well as equal in size.

4. Examples

In the examples that follow, we refer to isostatic block-and-hole frameworks, meaning that the structure is isostatic considered as a bar-joint framework; the panel-hinge analogue would have additional stresses of the type described in Section 3.1. The illustrations in this section often include Polydron (hence panel-hinge) models, because they are easy to build and understand at a glance, even when the analysis is actually made in terms of a bar-joint model.

4.1. Symmetry-isostatic frameworks

4.1.1. Strongly counting-balanced examples

It is straightforward to construct examples of strongly counting-balanced block-and-hole frameworks that are symmetry-isostatic. A *belted [k]-bipyramid* is a doubly coned [k]-prism (see Fig. 4(a) for a Schlegel diagram). When all square faces are capped, this structure becomes a triangulated sphere, the *belted and braced [k]-bipyramid* (Fig. 4(b)). A block-and-hole bar-joint framework can be made by alternate deletion and duplication of the equatorial vertices; the corresponding panel-hinge structure (Fig. 4(c)) has alternate central blocks and holes.

Consider the $\mathcal{D}_{3h}$-symmetric structure in Fig. 4(c). The three *holes* span the $\mathcal{O}_{3h}$ orbit of the group (a set of three objects that are exchanged by the principal C_3 rotation and fixed by the horizontal σ_h mirror plane). The three *blocks* span a second copy of the same orbit. Hence, the framework is actually strongly symmetry-
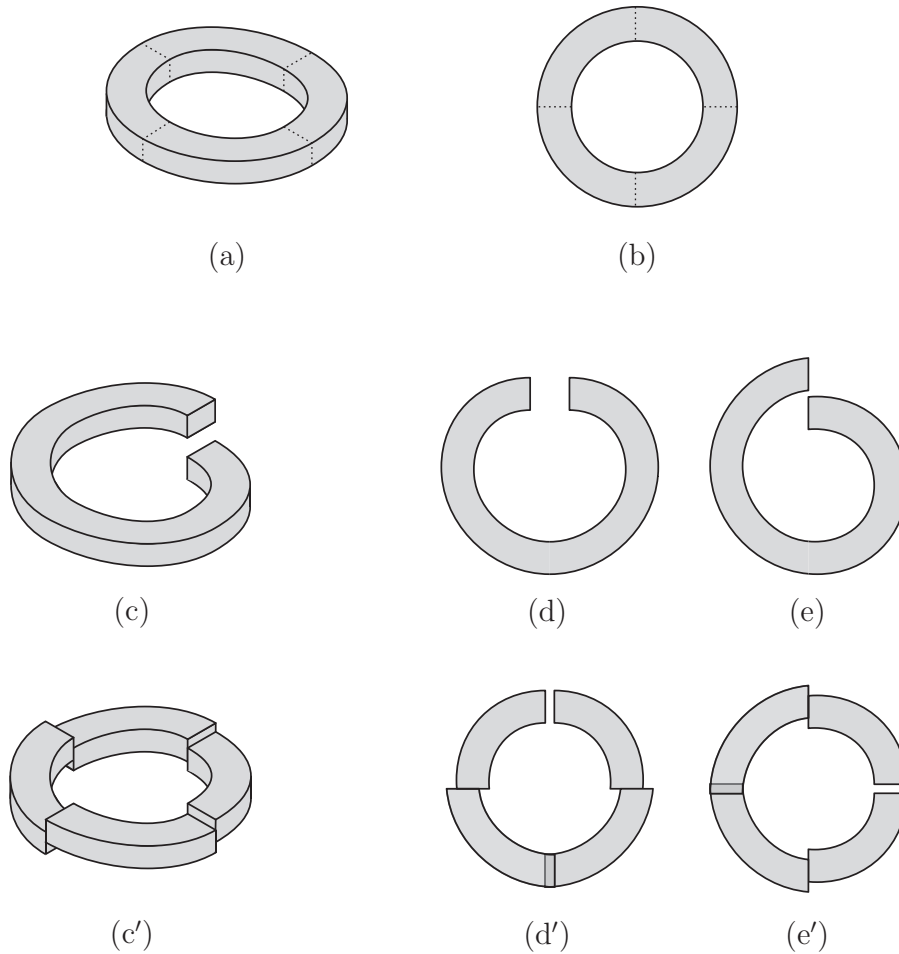
Fig. 3. A depiction of the extra local states of self-stress in a panel-hinge block-and-hole polyhedron. At a vertex, edges and panels come together so that a continuous ring of material is formed, although of infinitesimal extent. This ring is shown in isometric view in (a), and along a radius of the underlying object in (b): four potential 'cut' lines are shown. An independent set of three states of self-stress is here visualized by considering the shape the ring would take up if cut to relieve the internal stresses. In (c)–(e) the ring is cut in just one place, while in (c′)–(e′) the ring is cut in four places; it is clear from this that (d′) and (e′) form a pair, with one state of self-stress just the rotated version of the other. These states of self-stress are intrinsic: they cannot be relieved by bending around the hinges intersecting at the vertex.

balanced, with

$$\Gamma(v_{\mathrm{h}}) = \Gamma(v_{\mathrm{b}}) = A_1' + E'$$

and

$$\Gamma(e_{\mathrm{h}}) = \Gamma(e_{\mathrm{b}}) = A_1' + A_2' + 2E' + A_1'' + A_2'' + 2E'',$$

giving $(\Gamma(m) - \Gamma(s))_{\mathrm{BH}} = 0$ A similar result would be obtained for the corresponding derivatives of any $[4p + 2]$-bipyramidal structure where equatorial blocks and holes alternate. All are strongly symmetry-balanced in the point group $\mathcal{D}_{(2p+1)h}$.

However, it is easy to see that the $[4p]$-bipyramidal structures with the same block-hole alternation are finitely flexible, with a mechanism that destroys symmetry about the C_{2p} rotational axis and the horizontal mirror plane of the $\mathcal{D}_{(2p)h}$ point group (see Fig. 4(d), (e) for the case $p = 2$).

Another easy way to achieve a strongly symmetry-balanced framework is to use only *regular orbits* (Fowler and Quinn, 1986) of blocks and holes. A framework with point group $\mathcal{G}$ where every block and hole has trivial site symmetry has all block and hole orbits of size $|\mathcal{G}|$, has representations $\Gamma(v_{\mathrm{h}}) = \Gamma(v_{\mathrm{b}})$ and $\Gamma(e_{\mathrm{h}}) = \Gamma(e_{\mathrm{b}})$, and hence $(\Gamma(m) - \Gamma(s))_{\mathrm{BH}} = 0$.

4.1.2. Counting-balanced examples

There are also symmetry-isostatic block-and-hole frameworks which are counting-balanced, but not strongly counting-balanced.

One example of this type is obtained by perturbing the block-and-hole framework shown in Fig. 5 so that the mirror symmetry with respect to the σ_2 plane (and hence the half-turn symmetry) is destroyed, and only the mirror symmetry in the σ_1 plane survives. The perturbed framework is symmetry-balanced.

Another example of this type is shown in Fig. 6. This block-and-hole framework has only reflection symmetry, and is counting-balanced as a bar-joint framework. In this case, the framework is symmetry-isostatic, but not symmetry-balanced.

4.1.3. Counting-isostatic examples

Finally, it is also easy to construct counting-isostatic bar-joint block-and-hole frameworks that are not counting-balanced, but still symmetry-isostatic. Consider, for example, the $\mathcal{C}_3$-symmetric counting-isostatic framework shown in Fig. 7. With three blocks and only one hole, it is not counting-balanced. However, explicit calculations in the tabular form we have used before (see Fowler and Guest, 2000; Guest and Fowler, 2005; Fowler et al., 2016 for example) show that it is symmetry-isostatic (see Table 1).

4.2. Counting-isostatic but not symmetry-isostatic frameworks

We now consider examples of block-and-hole frameworks that are counting-isostatic, but have symmetry-detectable mechanisms and states of self-stress.
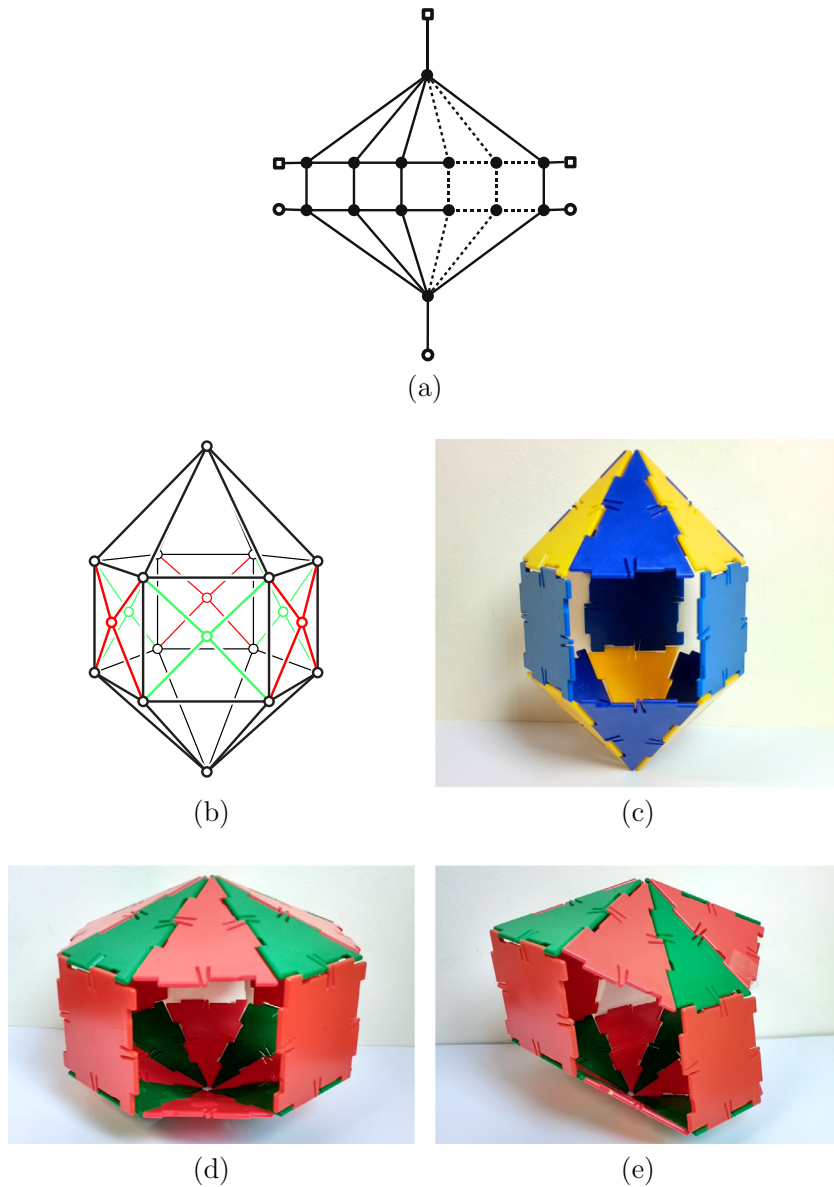
(a)

(b)

(c)

(d)

(e)

Fig. 4. Structures derived from belted [k]-bipyramids. (a) Schlegel-like diagram of a typical member of the belted bipyramid family. Hollow triangular and square symbols indicate parts of a composite vertex. (b) The corresponding triangulated sphere, the belted and braced [k] bipyramid with $k = 6$. (c) to (e) Polydron models of derived block-and-hole polyhedra: (c) An isostatic example with $k = 6$ and point group $\mathcal{D}_{3h}$; (d) A finitely flexible example with $k = 8$ and point group $\mathcal{D}_{4h}$; (e) A point on the path of the mechanism of structure (d).

Table 1
The mobility representation for the bar-joint block-and-hole example in Fig. 7, which is shown by calculation to be equal to the zero representation.

$\mathcal{C}_3$	E	C_3	C_3^2
$\Gamma(v_b)$	3	0	0
$-\Gamma(v_h)$	−1	−1	−1
	2	−1	−1
$\times \Gamma_T$	3	0	0
	6	0	0
$\Gamma(e_h)$	6	0	0
$-\Gamma(e_b)$	−12	0	0
$\Gamma(m) - \Gamma(s)$	0	0	0

4.2.1. Counting-isostatic examples

We begin with an example that is counting-isostatic, but not counting-balanced. The eponymous *Sarrus linkage* may be obtained from the spherical triangulation depicted in Fig. 8 and is shown in Fig. 9(a). It consists of six panels connected by hinges, and the

unique mechanism maintains top and bottom platforms in parallel alignment. It serves as a means of converting a partial circular motion into linear motion. Note that the Sarrus linkage relies on triplets of mutually parallel hinges.

We can analyse either the panel-hinge structure or its bar-joint equivalent, and will arrive at the same result, as in this case all vertices of the underlying triangulated sphere are incident with a hole, and hence there are no 'extra' states of self-stress for the panel-hinge version. We use the bar-joint version here. In full $\mathcal{C}_{2v}$ symmetry, we have $\Gamma(v_h) = 2A_1$, $\Gamma(v_b) = 2A_1 + A_2 + 2B_1 + B_2$, $\Gamma(e_h) = 4A_1 + A_2 + 2B_1 + 3B_2$, $\Gamma(e_b) = 4A_1 + 4A_2 + 4B_1 + 4B_2$, and hence $\Gamma(m) - \Gamma(s) = A_1 - B_1$. This analysis detects the fully symmetric mechanism that gives the linkage its defining property, and the counterbalancing B_1 state of self-stress (with the symmetry of a vector lying in the σ_1 plane). Hence, even in a geometry that is generic modulo the given $\mathcal{C}_{2v}$ symmetry, the Sarrus linkage would still move, though not with the desirable retention of parallel top and bottom panels. (Note that the structure shown
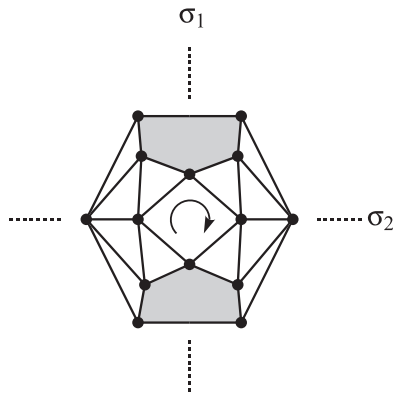
Fig. 5. A *counting-balanced*, but not *strongly counting-balanced*, block-and-hole framework with two pentagonal blocks and two holes with perimeters 4 and 6, respectively. The Schlegel diagram for the panel-hinge version shows the maximum possible $\mathcal{C}_{2v}$ symmetry, indicating the presence of a two-fold rotation and two perpendicular mirror planes.
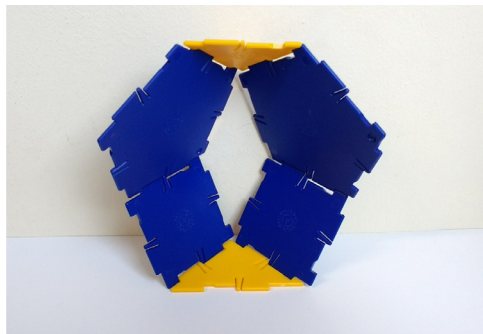

Fig. 6. A Polydron model of a block-and-hole structure of $\mathcal{C}_s$ (single reflection) symmetry for which the bar-joint representation is counting-balanced and symmetry-isostatic.

in Fig. 6 has lost one of the reflection planes and has become isostatic.)

In this case, swapping blocks and holes produces a physically different picture. The swapped structure is a variant of the Stewart-platform (Stewart, 1965; Dasgupta and Mruthyunjaya, 2000) in a singular configuration (see Fig. 10). This swap does not lead to a pure panel-hinge structure, as the hexagonal panel is now connected by hinges to the triangular panels, whereas the square panel is connected by pins and bars to the rest of the structure. However, the whole assembly can still be derived as a bar-joint framework from a triangulation of the sphere by our deletion/coning construction, with its mobility correctly accounted for, as again all vertices derived from the triangulation are incident
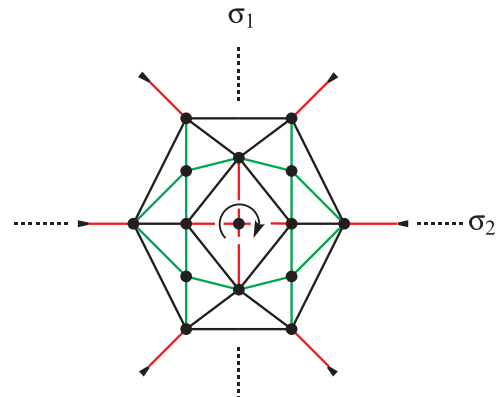
Fig. 8. A Schlegel-like diagram of a triangulated spherical polyhedron which yields the Sarrus linkage in Fig. 9(a) if the central vertex and the vertex 'at infinity' together with their incident edges (shown in red) are removed, and each vertex to four green edges is duplicated and coned over the same neighbours. Both the underlying polyhedron and the Sarrus linkage have maximum symmetry $\mathcal{C}_{2v}$, as indicated. Note that swapping the roles of green and red edges yields the Stewart platform in Fig. 10. (For interpretation of the references to colour in this figure legend, the reader is referred to the web version of this article.)

with holes. Symmetry counting in $\mathcal{C}_{2v}$ using (4) detects a *distortive* mechanism that would reduce the symmetry to $\mathcal{C}_s$, and also detects a totally symmetric state of self-stress. Hence the mechanism of this platform cannot be guaranteed to be finite, and in fact it is only infinitesimal.

4.2.2. Counting-balanced examples

Next we provide an example of a block-and-hole framework that is counting-balanced, but still has a symmetry detectable mechanism and state of self-stress (i.e., the framework is not symmetry-isostatic). Consider the $\mathcal{C}_{2v}$-symmetric block-and-hole framework shown as a Polydron model in Fig. 11. (See also Fig. 5.) It is counting-balanced, but not strongly counting-balanced, as it has two blocks (both 5-sided panels) and two holes (with perimeters of length 4 and 6, respectively). The calculation of characters in Table 2 shows that this framework has a totally symmetric mechanism and a corresponding state of self-stress of symmetry B_1.

4.2.3. Strongly counting-balanced examples

Finally, the most interesting situation arises when the framework is maximally balanced at the non-symmetric level, in the sense that it is strongly counting-balanced, but nevertheless has a symmetry-detectable mechanism and state of self-stress. This situation can arise when the orbit partitions of blocks and holes are mismatched, either in the distributions of orbit sizes, or of distin-
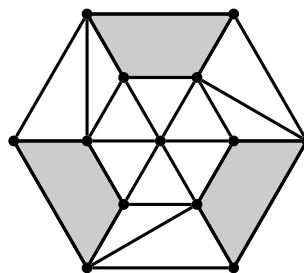
Fig. 7. A $\mathcal{C}_3$-symmetric isostatic block-and-hole framework which is not counting-balanced. (a) Polydron model and (b) Schlegel diagram of the panel-hinge structure. To make the bar-joint counting-isostatic structure, each square panel would need to be bicapped, the hollow triangles already being rigid.
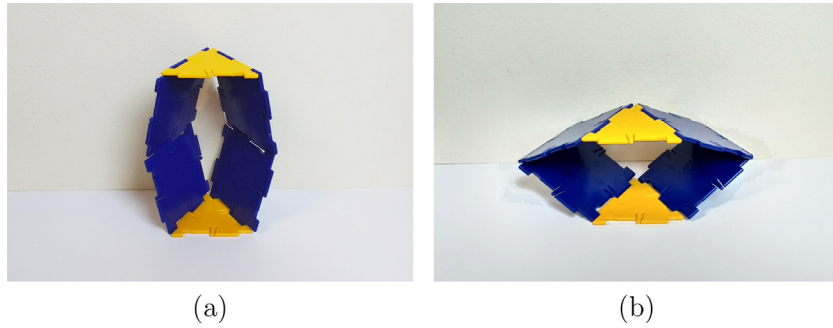
Fig. 9. A Polydron model of the Sarrus linkage (a) and a point on the path of its mechanism (b).
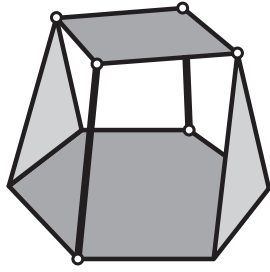

Fig. 10. A Stewart platform obtained by swapping blocks and holes in the Sarrus linkage shown in Fig. 9(a). Open circles indicate pin joints; there are two hinge joints connecting hexagonal and triangular panels.

Table 2
The mobility representation for the example in Fig. 11 is $\Gamma(m) - \Gamma(s) = A_1 - B_1$. The A_1 mechanism is finite. A swap of blocks and holes yields a finitely flexible framework whose motion preserves only the σ_1 mirror symmetry.

$\mathcal{C}_{2v}$	E	C_2	σ_1	σ_2
$\Gamma(v_b)$	2	0	2	0
$-\Gamma(v_h)$	-2	-2	-2	-2
	0	-2	0	-2
$\times \Gamma_T$	3	-1	1	1
	0	2	0	-2
$\Gamma(e_h)$	10	0	2	4
$-\Gamma(e_b)$	-10	0	-2	0
$\Gamma(m) - \Gamma(s)$	0	2	0	2

guishable orbits of the same size. Examples of both types are given by the three 'banana' structures illustrated in Fig. 12.

In case (a), selection of pairs of squares as respectively holes and blocks yields inequivalent orbits of the same size; in case (b) holes are exchanged by reflection in the symmetry plane, whereas the blocks are exchanged by the C_2 rotation. Again the orbits are of the same size, but are inequivalent. In case (c) the blocks span two orbits of size 1, whereas the holes are related by one of the sym-

metry planes and hence span one orbit of size 2. The explicit calculations in Table 3 show the mobility representations in all three cases.

In case (a) the detected mechanism and state of self-stress each have the symmetry of a rotation about an axis orthogonal to the principal axis. The blocks and holes span complementary halves of a four-orbit of the parent $\mathcal{D}_{4h}$ group. A swap of blocks and holes leads to a change of setting of the $\mathcal{D}_{2h}$ subgroup induced by the choice of half-orbits, but not to physically distinguishable mechanisms/states of self-stress.

Case (a) extends to the already mentioned case of belted [4k]-bipyramids, where blocks and holes belong to complementary orbits lying on either σ_v or σ_d planes, giving one symmetry-detectable mechanism and one state of self-stress for each k.

In case (b), holes and blocks each span one orbit. The mechanism is totally symmetric and the state of self-stress is symmetric under inversion only. A swap of blocks and holes gives a totally symmetric state of self-stress, implying the possibility of blocking the mechanism (now of B_g symmetry). In fact, the mechanism is clearly finite in the swapped framework.

In case (c), holes span a single orbit of size 2, but blocks span two of size 1. The mechanism has the symmetry of a vector across the C_2 axis, leading to $\mathcal{C}_s$ symmetry in the distorted structure; the state of self-stress is anti-symmetric with respect to both reflections, and therefore anti-symmetric in the lower symmetry group, indicating that the mechanism is finite. A swap of blocks and holes now leads to a physically distinct situation, with a $\mathcal{C}_2$-preserving mechanism, also finite.

4.3. Some limitations of symmetry counting: block-and-hole towers.

A well-studied class of block-and-hole structures are the *tower structures*, which contain a single block of size s and a single hole of size t, where the block may be considered as the 'ground', and the hole as the 'open top' of the tower (Finbow-Singh et al., 2012; Whiteley, 2014). A tower structure is (strongly) counting-balanced
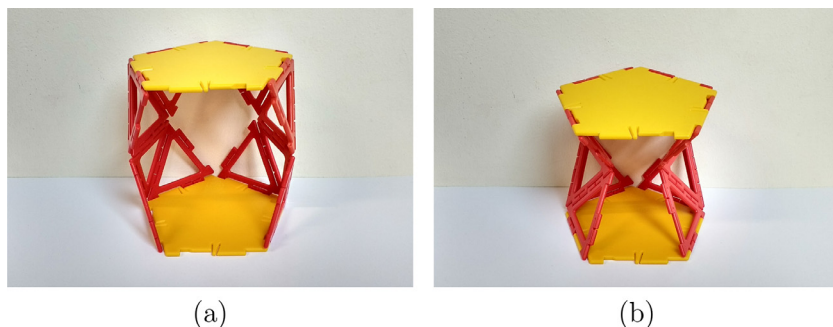

Fig. 11. A Polydron model of a finitely flexible panel-hinge structure with point group $\mathcal{C}_{2v}$ (a), and a point on the path of the mechanism (b).
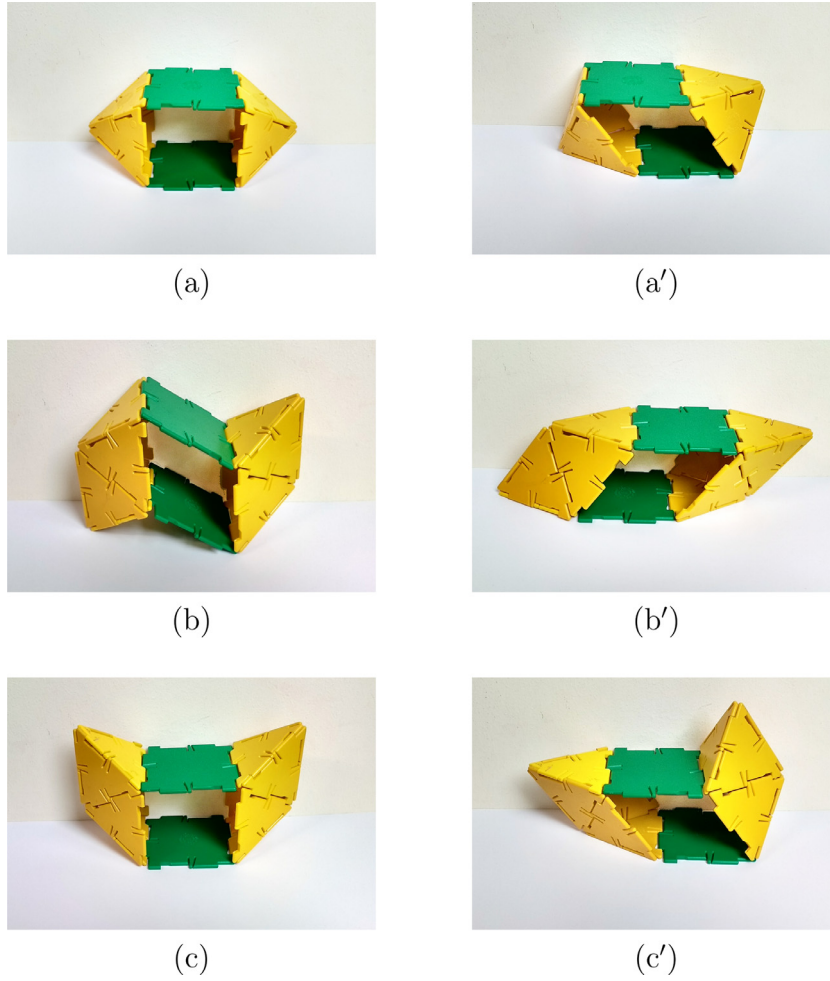
Fig. 12. Polydron models of finitely flexible symmetric block-and-hole structures that are strongly counting-balanced. For the structures in (a), (b) and (c), figures (a′), (b′) and (c′) show a point on the path of the corresponding mechanism.

Table 3
Calculations of mobility representations for the three structures shown as Polydron models in Fig. 12(a)–(c). Case (a): The mobility representation is $(\Gamma(m) - \Gamma(s))_{BH} = B_{3g} - B_{2g}$. A swap of blocks and holes yields the same representation with a different labelling. Case (b): Here $(\Gamma(m) - \Gamma(s))_{BH} = A_g - B_g$. The totally symmetric A_g mechanism is finite. A swap of blocks and holes yields a framework with a B_g mechanism (preserving $\mathcal{C}_i$ symmetry). This mechanism is not blocked by the A_g state of self-stress associated with the caps. Case (c): Here $(\Gamma(m) - \Gamma(s))_{BH} = B_1 - A_2$. The finite B_1 mechanism reduces the symmetry of the structure from $\mathcal{C}_{2v}$ to $\mathcal{C}_s$. A swap of blocks and holes leads to a finitely flexible framework whose motion preserves $\mathcal{C}_2$ symmetry.

Case (a)

$\mathcal{D}_{2h}$	E	$C_2(z)$	$C_2(y)$	$C_2(x)$	i	σ_{xy}	σ_{xz}	σ_{yz}
$\Gamma(v_b)$	2	0	2	0	0	2	0	2
$-\Gamma(v_h)$	−2	0	0	−2	0	−2	−2	0
	0	0	2	−2	0	0	−2	2
$\times \Gamma_T$	3	−1	−1	−1	−3	1	1	1
	0	0	−2	2	0	0	−2	2
$\Gamma(e_h)$	8	0	0	0	0	0	0	0
$-\Gamma(e_b)$	−8	0	0	0	0	0	0	0
$\Gamma(m) - \Gamma(s)$	0	0	−2	2	0	0	−2	2

Case (b)   **Case (c)**

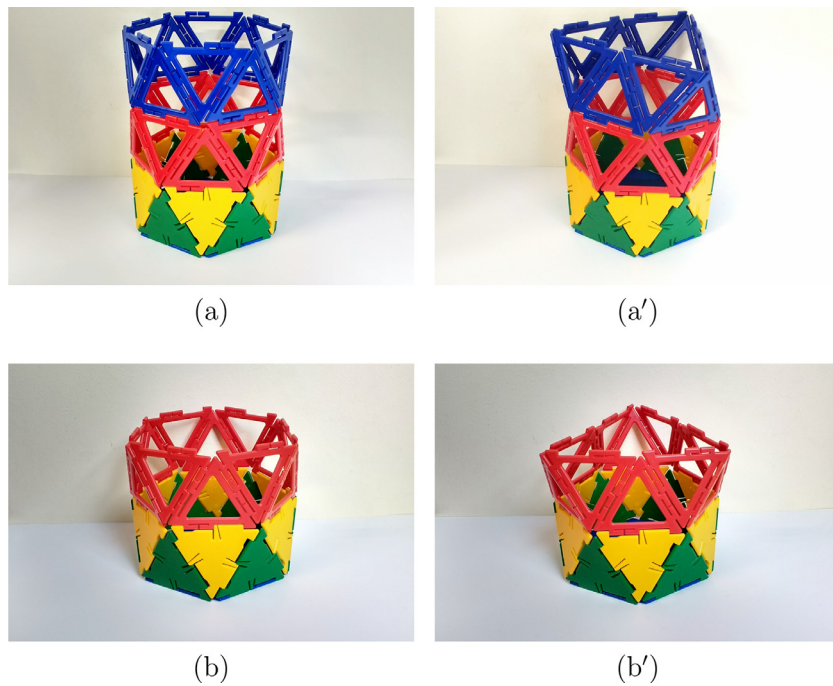| $\mathcal{C}_{2h}$	E	C_2	i	σ_h	$\mathcal{C}_{2v}$	E	C_2	σ_1	σ_2
$\Gamma(v_b)$	2	0	0	2	$\Gamma(v_b)$	2	2	2	2
$-\Gamma(v_h)$	−2	−2	0	0	$-\Gamma(v_h)$	−2	0	0	−2
	0	−2	0	2		0	2	2	0
$\times \Gamma_T$	3	−1	−3	1	$\times \Gamma_T$	3	−1	1	1
	0	2	0	2		0	−2	2	0
$\Gamma(e_h)$	8	0	0	0	$\Gamma(e_h)$	8	0	0	0
$-\Gamma(e_b)$	−8	0	0	0	$-\Gamma(e_b)$	−8	0	0	0
$\Gamma(m) - \Gamma(s)$	0	2	0	2	$\Gamma(m) - \Gamma(s)$	0	−2	2	0

Fig. 13. (a),(b) Polydron models of flexible tower structures with a hexagonal block and hole; (a′), (b′) points on the paths of the corresponding mechanisms.

iff the block and the hole are of the same size, say $s = t = k$. A tower constructed from a k-gonal panel by adding l layers of triangulated rings on top of it (as shown in Fig. 13) is called a [k, l]-*tower*. We can analyse the rigidity of [k, l]-towers within their largest possible symmetry group, $\mathcal{C}_{kv}$.

Suppose first that k is even. If l is odd, we obtain $(\Gamma(m) - \Gamma(s))_{\text{BH}} = B_2 - B_1$, and hence the structure has a symmetry-detectable infinitesimal mechanism and state of self-stress. This B_2 mechanism is in fact finite and deforms the triangular ring on the very top of the tower, reducing the point group of the structure to $\mathcal{C}_{(k/2)v}$. See Fig. 13(a) and (a′) for an illustration of the case $k = 6$ and $l = 3$. Note that the structure actually has further infinitesimal mechanisms, one for each of the layers $1, \ldots, (l - 1)$. However, for each $i = 1, \ldots, (l - 1)/2$, the infinitesimal mechanism in the $2i$th layer has an equi-symmetric state of self-stress in the $(2i - 1)$th layer below it and vice versa, and hence they all remain undetected by our working equation.

If both k and l are even, the [k, l]-tower is strongly symmetry-balanced, and hence symmetry-isostatic. Nevertheless, the structure again has a finite mechanism deforming the triangular ring on the very top of the tower. This is illustrated in Fig. 13(a) and (a′) for the case $k = 6$ and $l = 2$. However, this mechanism is paired with an equi-symmetric state of self-stress in the ring below it, and is hence undetectable with our working equation. In fact, as above, any [k, l]-tower, where k and l are even, actually has an infinitesimal mechanism and a state of self-stress for each of its layers. However, since l is even, none of these infinitesimal mechanisms or states of self-stress can be detected with our working equation.

Finally, it is easy to see that for all odd k, all [k, l]-towers with $\mathcal{C}_{kv}$ symmetry are strongly symmetry-balanced; in fact, these structures are isostatic.

5. Conclusions

The symmetry counting approach, together with a simple construction as bar-joint frameworks based on modification of spherical triangulations, has been shown to extend the information available from pure scalar counting for block-and-hole structures in typical cases. Symmetry also casts light on differences between bar-joint and panel-hinge realisations of such structures.

Various extensions beyond the simplest version of the construction as presented in Section 2 would be straightforwardly implemented. For example, in the construction we focussed on the case where no holes share a vertex of the original triangulation, but the symmetry mobility analysis also applies to at least the following more general structures. If two holes meet in just a single vertex (or in a finite set of vertices), we can augment the model by adding pin joints between the panels that meet at the vertices. If we allow holes to share an edge, we can consider the edge to act as a bar connecting the pin joints at the shared vertices.

The differencing technique for assigning $\Gamma(m) - \Gamma(s)$ is also applicable to over-braced and under-braced structures. In particular, we have used symmetry methods to analyse the structures that have been called 'perforated polyhedra' (Fowler et al., 2016). Three basic examples are obtained by the removal of six panels from the equator of a small rhombicuboctahedron and choosing one of three mutual rotations of tropical and equatorial layers. Although these can be treated (Fowler et al., 2016) using an explicit calculation of $\Gamma(m) - \Gamma(s)$ for a body-hinge structure, it would be perfectly possible to apply a bar-joint rendering of each. The objects are over-braced, with a count $m - s = -6$, corresponding to seven states of self-stress and a unique distortive mechanism. The underlying deltahedron in the present block-and-hole approach is of course isostatic, and as there are six holes and twelve blocks (all square faces of the body-hinge structure) the excess of states of self-stress arises from the excess of blocks over holes, but symmetry is needed to see that this net excess of 6 arises from 7 states of self-stress and 1 mechanism. The mechanism emerges in these particular examples as having the symmetry of the xyz spherical harmonic. Arguably, the block-and-hole approach gives a more transparent account of these intriguing structures.

There are many more examples that are covered by the block-and-hole paradigm.

References

Altmann, S.L., Herzig, P., 1994. Point-Group Theory Tables. Clarendon Press, Oxford.

Atkins, P.W., Child, M.S., Phillips, C.S.G., 1970. Tables for Group Theory. Oxford University Press.

Baker, D., Friswell, M.I., 2009. Determinate structures for wing camber control. Smart Mater. Struct. 18 (3), 035014.

Bujakas, V.J., Rybakova, A.G., 1998. High precision deployment and shape correction of multimirror space designs. In: Pellegrino, S., Guest, S.D. (Eds.), Proceedings of the IUTAM-IASS Symposium on Deployable Structures: Theory and Applications. Kluwer Academic Publishers, pp. 55–62.

Calladine, C., 1978. Buckminster fuller's 'tensegrity' structures and clerk mAxwell's rules for the construction of stiff frames. Int. J. Solids Struct. 14, 161–172.

Cauchy, A.L., 1813. Recherche sur les polyèdres - premier mémoire. Journal de l'Ecole Polytechnique 9, 66–86.

Ceulemans, A., Fowler, P.W., 1991. Extension of euler's theorem to the symmetry properties of polyhedra. Nature 353, 52–54.

Connelly, R., Fowler, P.W., Guest, S.D., Schulze, B., Whiteley, W., 2009. When is a pin-jointed framework isostatic? Int. J. Solids Struct. 46, 762–773.

Cruickshank, J., Kitson, D., Power, S., 2017. Journal of Combinatorial Theory. Series B 122, 550–577.

Dasgupta, B., Mruthyunjaya, T.S., 2000. The stewart platform manipulator: a review. Mech. Mach. Mach. Theory 35, 15–40.

Dehn, M., 1916. Über die starrheit konvexer polyeder. Math. Ann. 77, 466–473.

Finbow-Singh, W., Ross, E., Whiteley, W., 2012. The rigidity of spherical frameworks: swapping blocks and holes in spherical frameworks. SIAM J. Discrete Math. 26 (1), 280–304.

Finbow-Singh, W., Whiteley, W., 2013. Isostatic block and hole frameworks. SIAM J. Discrete Math. 27 (2), 991–1020.

Fowler, P.W., Guest, S.D., 2000. A symmetry extension of maxwell's rule for rigidity of frames. Int. J. Solids Struct. 37, 1793–1804.

Fowler, P.W., Guest, S.D., Schulze, B., 2016. Mobility of a class of perforated polyhedra. Int. J. Solids Struct. 85–86.

Fowler, P.W., Quinn, C., 1986. σ, π And δ representations of the molecular point groups. Theor. Chim. Acta 70, 333–350.

Gluck, H., 1975. Almost all simply connected closed surfaces are rigid. Geometric Topology, Lecture Notes in Mathematics 438, 225–239.

Grübler, M., 1917. Getriebelehre. Springer, Berlin.

Guest, S.D., Fowler, P.W., 2005. A symmetry-extended mobility rule. Mech. Mach. Theory 40, 1002–1014.

Guest, S.D., Fowler, P.W., 2007. Symmetry conditions and finite mechanisms. J. Mech. Mater. Struct. 2 (2), 293–301.

Katoh, N., Tanigawa, S., 2011. A proof of the molecular conjecture. Discrete Comput. Geomet. 45 (4), 647–700.

Kutzbach, K., 1929. Mechanische leistungsverzweigung. Maschinenbau, Der Betrieb 8, 710–716.

Maxwell, J.C., 1864. On the calculation of the equilibrium and stiffness of frames. Philosoph. Mag. 27, 294–299.

Maxwell, J.C., 1876. General considerations concerning scientific apparatus. South Kensington Museum Handbook to the Special Loan Collection of Scientific Apparatus. Chapman and Hall. Section 4.

Maxwell, J. C., 1890. On the Calculation of the Equilibrium and Stiffness of Frames. Collected Papers, XXVI. Cambridge University Press.

Miura, K., Furuya, H., Suzuki, K., 1985. Variable geometry truss and its application to deployable truss and space crane arm. Acta Astronaut. 12 (7–8), 599–607. https://doi.org/10.1016/0094-5765(85)90131-6.

Polydron, 2016. http://www.polydron.co.uk/.

Stewart, D., 1965. A platform with six degrees of freedom. Proc. Inst. Mech. Eng. 180 (1), 371–386.

Whiteley, W., 1988. Infinitesimally rigid polyhedra II: modified spherical frameworks. Trans. AMS 306 (1), 115–139.

Whiteley, W., 2014. Fragmentary and incidental behaviour of columns, slabs and crystals. Philosoph. Trans. R. Soc. A 372 (2008), 1–20.